

# Assessment of weld quality of aerospace grade metals by using ultrasonic matrix phased array technology

Jeong K. Na<sup>a</sup> and Sean T. Gleeson<sup>b</sup>

<sup>a</sup>WYLE Aerospace Group, 2700 Indian Ripple Road, Dayton, OH 45440

<sup>b</sup>EWI, 1250 Arthur E. Adams Drive, Columbus, OH 43221

## ABSTRACT

Advantages of two dimensional electronic ultrasonic beam focusing, steering and scanning with the matrix phased array (MPA) technology has been used to visualize the conditions of resistance spot welds in auto vehicle grade advanced high strength steel carbon steels nondestructively. Two of the commonly used joining techniques, resistance spot welding and resistance seam welding, for thin aerospace grade plates made of aluminum, titanium, and stainless steels have also been inspected with the same MPA NDE system. In this study, a detailed discussions of the current MPA based ultrasonic real time imaging methodology has been made followed by some of the NDT results obtained with various welded test coupons.

**Keywords:** Matrix Phased Array (MPA) Ultrasonic Technology, Resistance Spot Weld, Resistance Seam Weld, Real Time Ultrasonic Imaging

## 1. INTRODUCTION

The technique of using a matrix of ultrasonic transducer elements differs in principle from single element or linear phased array ultrasonic inspection methods because the arrangement of the piezoelectric elements in a matrix array inherently produces two dimensional position data. Because position information is always available with reference to the array's elements, collected data can always generate as a C-scan image. This inherent electronic scanning nature differentiates the MPA technology from single element or linear phased array ultrasonics where both techniques require a mechanical raster scanning mechanism to index position data to produce a C-scan image<sup>1,2</sup>.

Since a C-scan provides a top down view, it is arguably the most intuitive way to display ultrasonic data. Having ultrasonic data continuously displayed in a C-scan format has the advantage of simplifying the interpretation of the information which enables defect detection to be automated or allows operators with general knowledge of ultrasonic inspection techniques to assess. Because the size, shape, element size and element pitch of the array is known, the size of features detected in the C-scan image can estimated using well established feature detection software. Once a feature is detected, calculations on the feature can be quickly performed allowing area, length, width etc., to be available in real time. This technique is designed to free the end user from complicated analysis of non-destructive testing information by presenting this data in a form which is intuitive quantitative in nature.

## 2. MATRIX PHASED ARRAY METHOD

The main advantages of MPA systems are the beam steering capability in 3-D space, beam focusing in spherical, elliptical, or linear patterns, focusing at different depths and skew angles using the same wedge, and two-plane steering capability for simultaneous variation of both the refracted and skew angles of the ultrasonic beam.

It was recognized that there was a need to develop a new ultrasonic inspection system for defect detection in thin metal sheets, especially with specimens with a lower uncertainty level in determining defect size and location. To reduce the cost and time for developing a reliable high frequency MPA probe with an appropriate acoustic delay line that provides an optimum propagation distance for the ultrasonic beam to be steered and focused on to part interface, computational modeling and simulation methods were performed. Commercially available CIVA modeling and simulation package was used for this work<sup>3</sup>.

To design the appropriate ultrasonic transducer, it is necessary to define material parameters such as material thickness and defect size. Initially, the system was first developed for inspection of resistance spot welds used on car bodies. A literature review and discussions with clients in the automotive industry revealed that the majority of spot weld applications are for materials in the thickness range of 0.6 to 2 mm having a nominal weld diameter of 5 to 7 mm. Some initial beam modeling calculations were performed to determine general parameters for a probe that would be capable of inspecting spot welds in the targeted range. Figure 1 shows a schematic drawing of the 100-element MPA probe designed by the beam modeling tools. Consideration was also given to current MPA instrumentation capabilities. Several MPA instruments on the market today have a maximum limit on the number of elements in the order of 128 with a capability to activate up to 32 channels simultaneously.

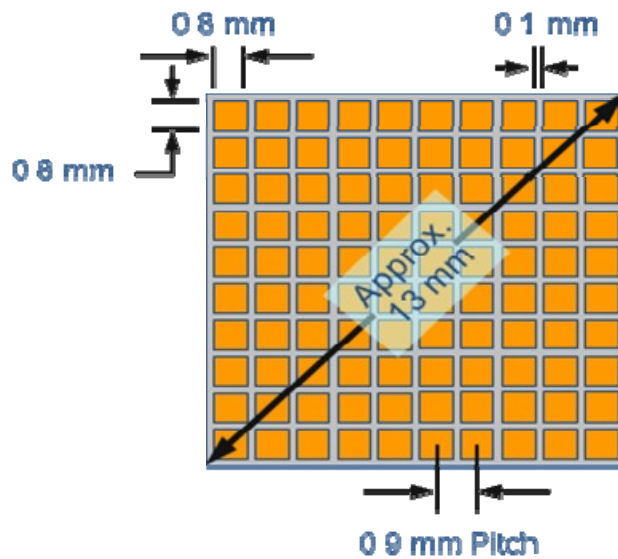


Figure 1. Schematic drawing of a high frequency matrix phased array probe element,  $f = 15$  MHz.

To achieve good focusing at a depth of 0.6 mm, it was required for the probe to have a physical delay distance between the probe element and the surface of part. Since water can offer the ability to conform to surface deformations caused by the welding electrodes, the delay line tip was assumed to be filled with water and the simulated images in Figure 2 show beam profile results using a 3x3 aperture at different water path lengths. By observing these images, it can be seen that water path length of 18 mm produces a narrow beam with minimum side lobes. The quality of ultrasonic beam that passes through the water and metal interface at a different water path length was simulated with a 3x3 aperture. It turned out that the water path length 18 mm gives the best beam focusing effect with minimum side lobes.

Based on the modeling result shown in Figure 2, a rod shaped probe was designed and fabricated. The active array is mounted at the end of the probe tip and the delay line is designed to be screwed on to the end. The cavity of the water column is supposed to be filled with water before it is screwed on the probe housing.

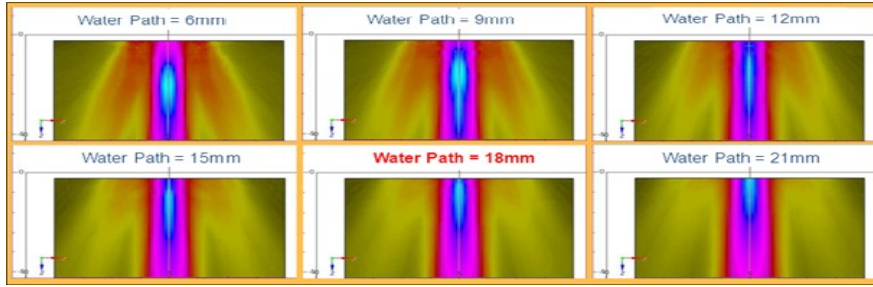


Figure 2. Modeling results of the water path lengths for a focused ultrasonic beam at the interface of two 2 mm metal sheets.

### 3. APPLICATION TO RESISTANCE SPOT WELDS

The NDE system was first designed with intention of inspecting resistance spot welds on automotive bodies made of thin high strength carbon steels. Weld conditions of automotive parts have been tested destructively by using a hammer and a screw driver or chisel. Destructive testing of 4,000-5,000 welds on a medium size vehicle takes not only long time and intensive labor but also generates scrap metals estimated to be approximately \$2M a year per plant. A reliable nondestructive inspection process can help reduce destructive testing as well as quality of vehicles.

#### 3.1 No-weld at interface

Figure 3 provides illustrations of test results derived from analyzing a no-weld condition using the MPA system. In this figure, because no fused weld nugget exists at the interface, ultrasonic beams do not travel through interface, but rather reflect back to the probe from the interface.

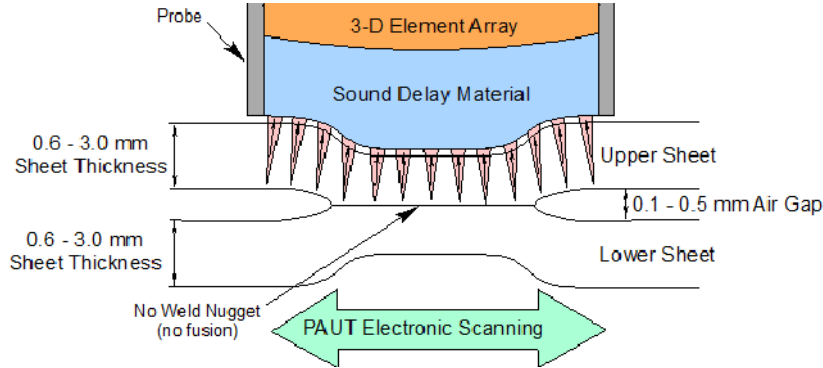


Figure 3. Ultrasonic beam launching from 3-D MPA probe through the interface with no weld.

Figure 4(a) illustrates diagrammatically the direction and relative strength of each sound wave as it reflects from interface. In this figure, a thinner line represents loss of elastic energy as the sound wave interacts with material and interface. The reflected signals designated as circled 1, 2, 3, 4, and 5 correspond to the peaks shown in the A-scan representation in Figure 4(b) wherein signal 1 represents the first reflection from the top surface of upper sheet, signal 2 represents the first reflection from interface, signal 3 represents the second reflection from interface, signal 4 represents the third reflection from interface, and signal 5 represents the fourth reflection from interface. The horizontal line drawn through signal 1 (Gate #1) represents the surface gate and the horizontal line drawn through signal 2 (Gate #2) represents the interface gate.

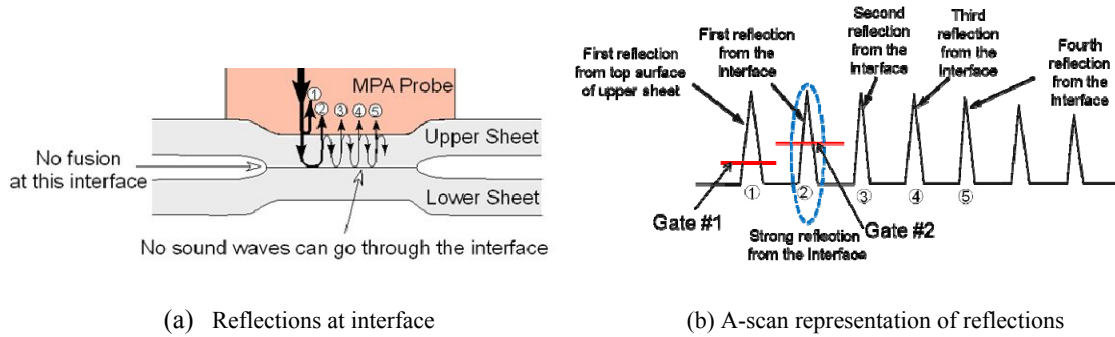


Figure 4. Multiple reflections of ultrasonic beam from the interface when no weld nugget is formed at the interface.

### 3.2 Weld at interface

Figure 5 provides illustrations of test results derived from analyzing a good spot weld condition. In this figure, ultrasonic beams travel through the weld nugget and reflect back to the probe from the backside of lower sheet.

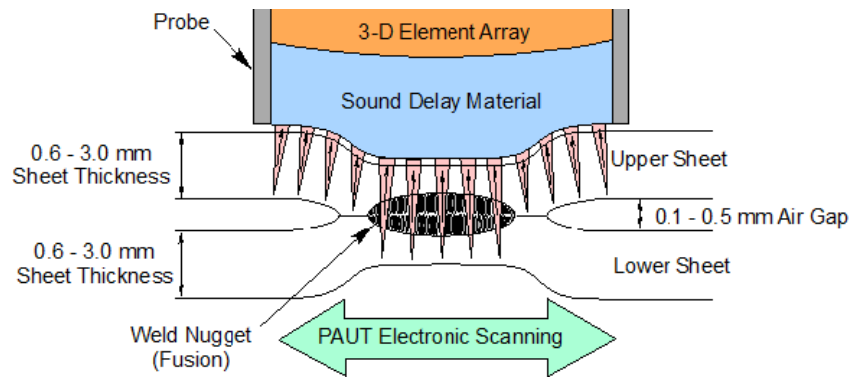


Figure 5. Ultrasonic beam launching from 3-D MPA probe through the interface with a well fused weld nugget at the interface.

Drawings in Figure 6 illustrate diagrammatically the direction and relative strength of each sound wave as it transmits through interface. Again, a thinner line in Figure 6(a) represents loss of acoustic energy as the sound wave interacts with material and interface. The reflected signals designated as circled 1, 2, and 3 correspond to the peaks shown in the A-scan representation in Figure 6(b). The horizontal line drawn through signal 1 represents a surface gate and the horizontal line between signals 1 and 2 represents an interface gate.

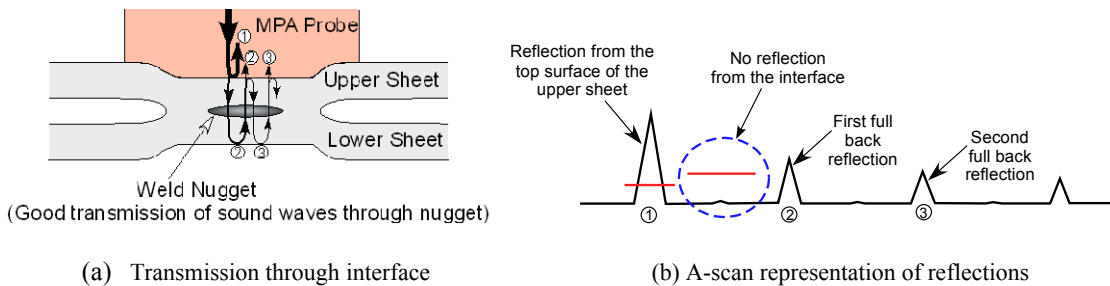


Figure 6. Multiple reflections of ultrasonic beam through the interface when well-fused weld nugget formed at the interface.

### 3.3 Ultrasonic image processing

Based on the ultrasonic energy transmission and reflection at interface, the system uses two adjustable electronic gates to filter out all unwanted ultrasonic signals. The two signals that pass through the two gates are either the front surface signal from the top side of the first sheet or the reflected signal from the interface. The first gate (Gate #1) is called the "surface gate" and the second gate (Gate #2) is called the "interface gate". The current MPA system measures the ratio of signal amplitude between Gates #1 and #2. Depending on the value of the ratio, Gate #2 amplitude divided by Gate #1 amplitude, four different colors, orange, yellow, green, and blue are assigned to form a C-scan image. When the amplitude ratio is zero, orange color is assigned, while blue is assigned for the ratio value of  $\sim 0.8$  or higher. Images in Figure 7 show the color coded C-scan results of the resistance spot welded part shown in Figure 8. The weld diameter was estimated to be 5.6 mm and 5.5 mm for weld #5 and weld #6, respectively.

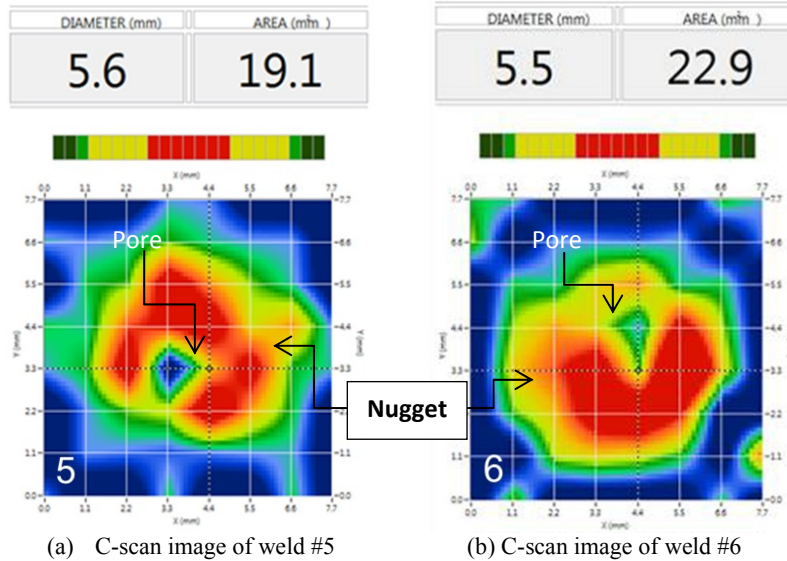


Figure 7. Ultrasonic C-scan images of resistance spot welds with pores.

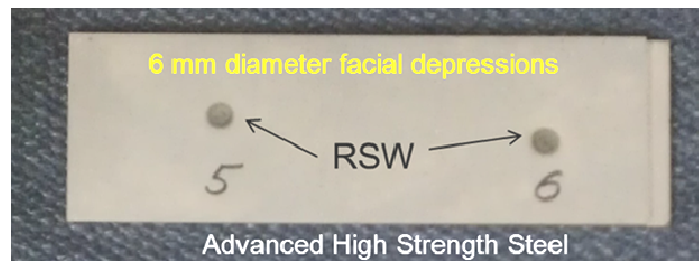


Figure 8. Photo of the resistance spot weld test specimen, two-0.7 mm stack, used for the images in Figure 7.

The same part used for ultrasonic imaging was cut across the width of the specimen to inspect the nugget size and porosity destructively. The results are shown in Figure 9. Both welds #5 and #6 have about 5.6 mm of nugget diameter and the pore in weld #5 is estimated to be 0.85 mm, while the pore in weld #6 is estimated to be 0.7 mm. When compared with the diameter estimations shown in Figure 7 images, one can notice that the ultrasonic data for the diameter matches very close to the destructive results. In addition to the accurate nugget diameter estimation, the relative sizes of pores can be estimated from the images as well. Qualitatively speaking, the pore in weld #5 is larger than the pore in weld #6 as measured from the cross-sectional macro images in Figure 9.

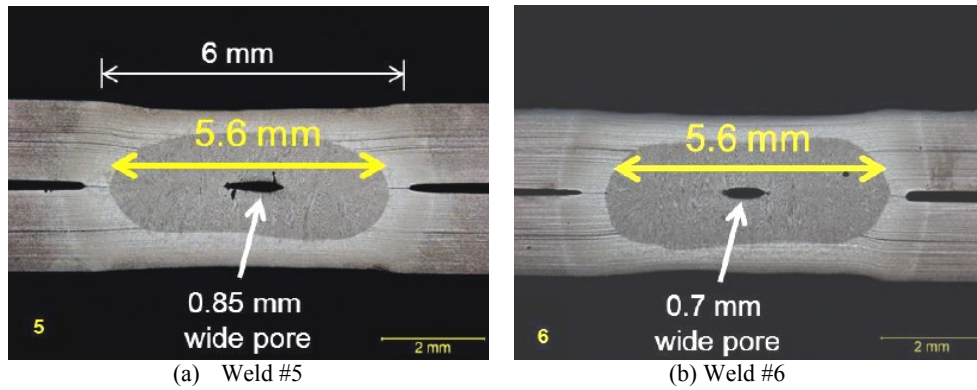


Figure 9. Cross-sectional macro images of pores in the spot welds used for the ultrasonic imaging in Figure 7.

#### 4. APPLICATION TO AIRCRAFT MATERIALS

Test specimens made of aircraft grade stainless steel, aluminum and titanium alloys were welded by using two different joining processes: resistance spot welding for stainless steel plates and resistance seam welding for aluminum and titanium plates. NDE system used for the carbon steel plates was used without any modifications. Ultrasonic gate positions were adjusted according to the thicknesses of the specimens.

##### 3.1 Resistance spot welds of stainless steel

Figure 10 shows the images of nuggets formed between two 1.6 mm thick aircraft stainless steel plates. Both images of welds #1 and #3 show pores in the welds with average weld diameters of 6.3 and 7.0 mm, respectively. Weld #2, however, has a smaller diameter, 5.8 mm, but no pore in the weld.

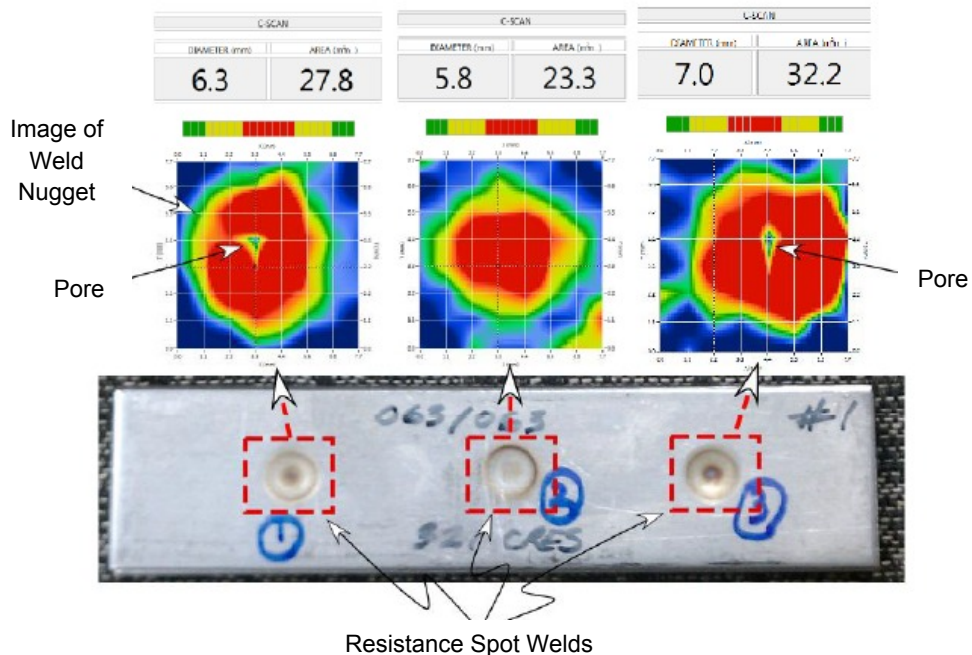


Figure 10. Images of resistance spot welds in aircraft grade stainless steel plates.

### 3.2 Resistance seam welds of aluminum and titanium alloys

For this testing, the welded area on the part was divided into seven sections as indicated in the lower portion of the image shown in Figure 11. The composite image at top was made by putting together all seven individual C-scan images taken from each grid point marked on the specimen. Area in dark orange color represents the fused section in the interface of the two 1 mm thick plates. Similarly, the resistance seam welded test specimen made of two 0.5 mm thick titanium plates was tested and result is shown in Figure 12. Qualitatively speaking, based on the two ultrasonic images, the fused area of titanium is not as uniform as the aluminum test specimen. It is clear that the welded section of titanium is narrower than aluminum sample and no-fused spots are visible.

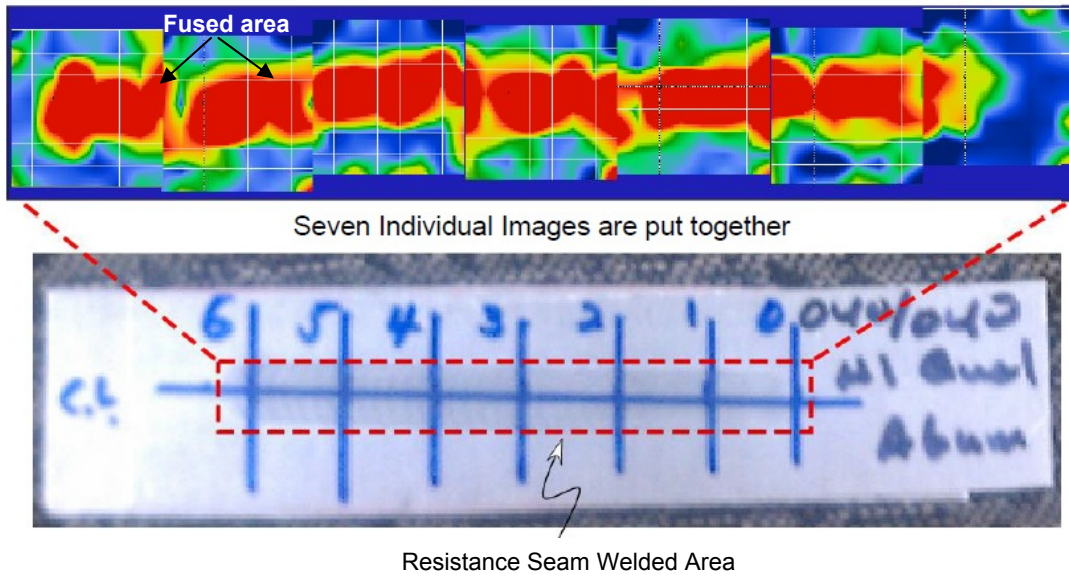


Figure 11. Composite image of resistance seam weld made on two 1 mm thick aircraft grade aluminum plates.

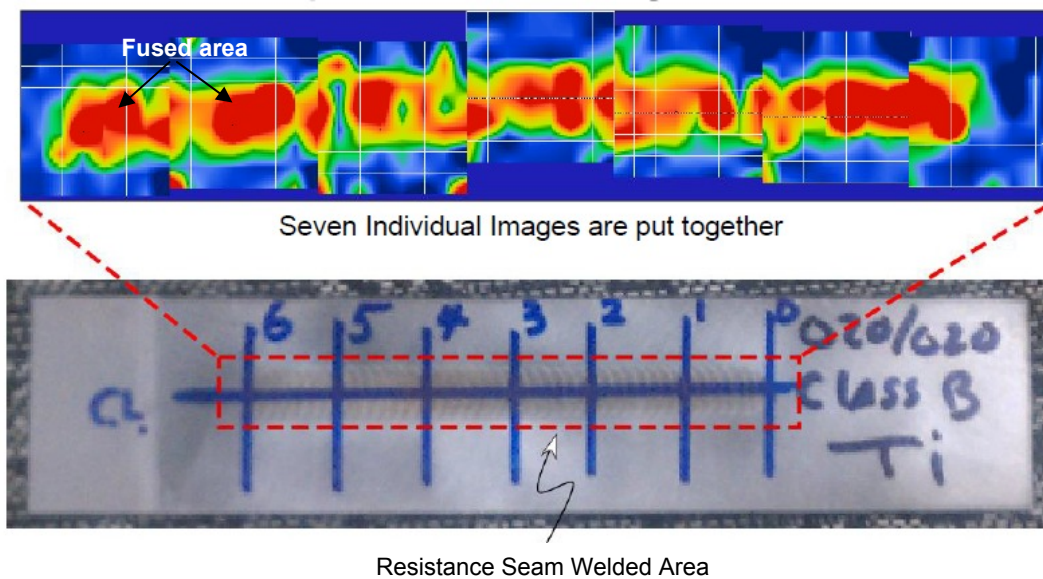


Figure 12. Composite image of resistance seam weld made on two 0.5 mm thick aircraft grade titanium plates.

## 5. SUMMARY AND CONCLUSION

A matrix phased array ultrasonic imaging system has been developed and tested to evaluate quality of welds made on auto vehicle quality high strength steel plates and quality of welds on aircraft grade stainless steel, aluminum and titanium plates. The main advantage of inherent two dimensional scanning capability of MPA technology was incorporated with an imaging algorithm using two gates. The ratio of the ultrasonic signal amplitudes measured through the two gates is represented with various colors to form a C-scan image for an easy interpretation. The average diameter of the nugget is estimated based on the C-scan image and the number is displayed on the screen. This dual gate concept works well for resistance seam welds to estimate the width of fused section and overall weld quality. It is envisioned that the same MPA NDE system can be used to inspect quality of laser welds, brazing and adhesively bonded parts.

## ACKNOWLEDGEMENTS

This work was internally funded and conducted at EWI.

## REFERENCES

- [1] J. Na and R. Spencer, "Design and Development of High Frequency Matrix Phased Array Ultrasonic Probes", *Review of Progress in Quantitative Nondestructive Evaluation*, Vol. 31A (2011).
- [2] Sean Gleeson, Gavin Dao and Jeong K. Na, "In-situ Weld Quality Inspection with Matrix Phased Array (MPA) Ultrasonic Technology", *Review of Progress in Quantitative Nondestructive Evaluation*, Vol. 33A (2013).
- [3] J. Na and Sean Gleeson, "Matrix Phased Array (MPA) Imaging Technology for Resistance Spot Welds", *Review of Progress in Quantitative Nondestructive Evaluation*, Vol. 33A (2013).